Temporal Evolution and Strength of Neural Activity in Parietal Cortex during Eye and Hand Movements

Alexandra Battaglia-Mayer, Massimo Mascaro and
Roberto Caminiti

Dipartimento di Fisiologia umana e Farmacologia,
Università di Roma "La Sapienza", 00185 Rome, Italy

The role of area 7a in eye–hand movement was studied by recording from individual neurons while monkeys performed 7 different tasks, aimed at assessing the relative influence of retinal, eye, and hand information on neural activity. Parietal cell activity was modulated by visuospatial signals about target location, as well as by information concerning eye and/or hand movement, and position. The highest activity was elicited when the hand moved to the fixation point. The population activities across different memory tasks showed common temporal peaks when aligned to the visual instruction (visuospatial peak) or Go signal (motor peak) for eye, hand, and coordinated eye–hand movement. The motor peak was higher for coordinated eye–hand movement, and it was absent in a No-Go task. Two activation maxima were also observed during visual reaching. They had the same latency of the visuospatial and motor peaks seen in the memory tasks. Therefore, area 7a seems to operate through a common neural mechanism underlying eye, hand, or combined eye–hand movement. This mechanism is revealed by invariant temporal activity profiles and is independent from the effector selected and from the presence or absence of a visible target during movement. For comparative purposes, we have studied the temporal evolution of the population activity in the superior parietal lobule (SPL) during the same reaching tasks and during a saccade task. In SPL, the population activity was characterized by a single peak, time locked to the Go signal for eye, hand, or combined eye–hand movement. As in IPL, the time of occurrence of this peak was effector independent. The population activity remained unchanged when the position of the eye changed, suggesting that SPL is mostly devoted to the hand motor behavior.

Keywords: eye–hand coordination, eye–hand temporal coupling, inferior parietal lobule, onset time of neural activity, reaching, superior parietal lobule

Introduction

In the cerebral cortex, eye and hand movements to visual targets are encoded within a distributed system including different parietal and frontal areas. These are linked by reciprocal corticocortical connections that define a gradient of visual, eye, and hand information critical for localizing objects of interest and for reaching toward them (for a recent review, see Battaglia-Mayer and others 2003). At neural level, these issues have mostly been studied through the analysis of the contribution provided by different areas of the superior parietal lobule (SPL) and by motor and premotor cortices (Battaglia-Mayer and others 2003) in the frontal lobe, although the analysis of the relationships between cell activity and reaching in behaving monkeys began in the inferior parietal lobule (IPL;

Hyvärinen and Poranen 1974; Mountcastle and others 1975). In these seminal studies, as well as in later ones (Blum 1985; MacKay 1992), the relative contribution of visual, eye, and hand signals to neural activity during reaches to visual targets has not been assessed. Therefore, it remains undetermined whether or not different information influences individual cells and, if so, to what extent they are combined in IPL neural activity. The relative contribution of different signals and the temporal relationships of cell activity with different behavioral events are critical issues in a cortical area where individual neurons display, among others, visual, oculomotor, and arm movement–related modulation. Furthermore, answering this question might facilitate understanding the dynamic mechanisms underlying a very common type of daily behavior, which occurs when the hand moves toward the fixation point (FP), that is, where selective attention is allocated at any given instant.

During visual reaching, although the onsets of eye and hand electromyogram (EMG) activities overlap in time (Biguer and others 1982), the eye moves toward and lands on visual targets well before the hand leaves its initial position. Therefore, reaches are made toward the newly achieved eye position, with the image of the hand on the retina moving from the periphery of the visual field to the fovea. Under these circumstances, cell activity during hand reaction time (RT) could be influenced by the co-occurring saccade, whereas vision of the moving hand might per se stimulate parietal visual neurons with motion sensitivity, such as those with opponent vector organization (Mountcastle and others 1981). Finally, when the hand attains the target, visual and/or eye position signals, which are known to exert powerful effects on virtually all classes of IPL neurons (Andersen and Mountcastle 1983; Andersen 1995), can contribute to neural activity, together with hand position information.

In the present manuscript, we illustrate the results obtained from the quantitative analysis of a large population of neurons in area 7a, studied through a multitask approach consisting of different visual and oculomanual tasks. Special attention was devoted to memory tasks because they facilitate the evaluation of the influence on neural activity of visuomotor instruction signals (ISs) and of eye, hand, or coordinated eye–hand movement performed in the absence of visual targets. Overall, the tasks adopted were aimed at 1) identifying the relative influence and weight of visual, eye, and hand information on neural activity; 2) evaluating if and to what extent a combination of signals occurred at single-cell level; and 3) elucidating the temporal dynamics of neural activity relative to eye–hand movement. For comparative purposes, the temporal relationships between neural activity and behavioral events during reaches to foveated and extrafoveal targets have been

contrasted to those obtained from SPL areas PEc and V6A, where cell activity had previously been recorded in the same tasks (Battaglia-Mayer and others 2000, 2001).

Materials and Methods

Animals, Apparatus, and Tasks

Two rhesus monkeys (*Macaca mulatta*, body weights 4.3 and 6.1 kg) were used in this study. They were the same animals used in the study of Battaglia-Mayer and others (Battaglia-Mayer and others 2005), to which the reader is referred for a more detailed description of the methodological approaches used. The monkeys sat on a primate chair with head fixed, and the eyes 17 cm in front of a 21 inches touch-sensitive (MicroTouch Systems, Wilmington, MA) computer monitor used to display the tasks and control hand position.

Monkeys performed 7 different tasks in total darkness. All arm movements were made with the hand contralateral to the hemisphere of recording. Arm and/or eye movements originated from a central position (Fig. 1*a*) and were directed toward 8 peripheral locations located on a circle of 7.5 cm radius (23.8° visual angle). All visuomotor tasks (Fig. 1*b–d*) started with the presentation on the center of the workspace of a red circle (subtending 1.5° visual angle) that the animal had to touch and fixate for a variable control time (CT, 1–1.5 s). At the end of the CT, in 2 reaction-time reaching tasks ("reaching" and "reach-fix"; Fig. 1*b,c*), a peripheral red target (subtending 1.5° visual angle) was lit. In the reaching task (Fig. 1*b*), the animals had to move the eyes (e) and the hand (h) to the target, within given RT and movement time. Due to the overlap of the onset times (OTs) of EMG activity in the eye and limb muscles during reaching (Biguer and others 1982), the time elapsing from presentation of the visual target to end of hand movement was divided into 4 distinct epochs, with the following temporal order (see Fig. 1*b*): RTeh (upper limit 400 ms) interpreted as reflecting preparation for both eye and hand movements; MTe (upper limit 600 ms) referring to the time of eye movement; RTh (upper limit 500 ms) reflecting preparation for hand movement only (at that time the eyes are already on the target, as a result of animals' natural behavior); MTh (upper limit 800 ms) referring to hand movement. At the end of the trial, animals were required to keep the eye and the hand immobile on the target for a variable target holding time (THT, 1–1.5 s.). This task was used to assess the relationships between cell activity and coordinated eye/arm movement to visual targets, as well as static holding on them. To dissociate hand- from eye-movement signals, in the reach-fix task (Fig. 1*c*), animals only moved the hand to the target and kept it there for a variable hand target holding time (THTh) while maintaining central fixation for the entire duration of the trial. Therefore, in this task, the sequence of temporal epochs after presentation of the visual target was as follows: RTh, MTh, THTh. The RTh as defined in the reaching and in the reach-fix task reflects preparation for hand movement with the eye on the visual target (reaching) or at the center (reach-fix). Time limits imposed to different epochs were as in the reaching task. In the 3 "memory" and in the "No-Go" tasks (Fig. 1*d*), a visual IS, consisting of a color square (1° visual angle), was presented for 300 ms at the end of the CT in 1 of 8 peripheral locations. After a variable memory delay (1–3 s), the center light went off, as Go signal. Depending on the color of the IS (blue, green, yellow, purple), the animals were required to make coordinated eye–hand movements (blue IS, "memory reach"), hand movements (green IS, "memory reach-fix"), eye movements (yellow IS, "memory eye") to the memorized target locations, or not move (purple IS, No-Go) for the entire duration of the trial. After the Go signal, the epochs sequences of memory reach and memory reach-fix were the same as in the reaching and in the reach-fix task, respectively (Fig. 1*b–d*). In the 3 tasks where the IS called for movement, at the end of this, the animals had to maintain the eye (memory eye), the hand (memory reach-fix), or both (memory reach) on the memorized target location for a variable THT (1–1.5 s). In these tasks, the influence of signals concerning future individual or combined eye–hand movement and position was studied in absence of visual stimulation. The No-Go task was used to assess, during attentive fixation at the center of the workspace, the influence on cell activity of peripheral visual stimuli that were presented at the same locations as in the previous tasks, but that

did not require any future movement. In each task, the 8 peripheral stimuli were presented in a pseudorandom order and during 4 repetitions. We have evidence from quantitative analyses done in the past, and from recent literature as well (Merchant and others 2001), that this does not significantly affect results. In any case, this limited number of repetitions was necessary to make the multitask experiment feasible. A "visual fixation task" (Fig. 1*e*) was used to determine visual responsiveness of individual neurons. A FP was presented at the center of the workspace. The monkeys fixated on FP and kept a key-down with the hand for a variable CT (1–1.5 s). A visual stimulus was initially presented in a stationary fashion in 1 of 16 locations (at 22.5° angular intervals), for a variable time (0.5–1 s), and then moved from the periphery of the visual field inward (IN) toward the fovea and outward (OUT) from the fovea to the periphery. At the end of the fixation time, the visual stimulus was extinguished, and the animal had to detect a 90° rotation of the FP, by releasing the telegraph key (key-up). Stimuli consisted of white solid bars (3.27° × 7.60°) and were moved at constant speed (25°/s) during attentive fixation. Visual stimuli were presented up to 30° eccentricity. All tasks were performed separately, in a block design fashion, without a specific order in the sequence of their presentation.

Behavioral Control

Eye position signals were recorded by using implanted scleral search coils (1° resolution) and sampled at 100 Hz (Remmel Labs, Ashland, MA). Fixation accuracy was controlled through circular windows (3.5° diameter) around the targets. Accuracy of eye fixation and movement across different tasks are shown in Figure 1*f,g*. This window size was chosen by considering that eye movements to memorized locations are typically hypometric when made downward, and hypermetric when directed upward, as shown in Figure 1*g*. Therefore, for successful fixation at the movement end points, a certain amount of tolerance was necessary. Eye velocity was calculated in off-line analysis. The OT and the end of the saccade were defined as the times when eye velocity exceeded or fell, respectively, 50°/s, for at least 30 ms. Hand position (Fig. 1*h,i*) was monitored through the touch screen, with 0.28 × 0.3 mm (1 screen pixel) resolution. Hand accuracy was controlled through 3 cm diameter circular windows (10° visual angle), at the origin and end point of movement.

Neural Recording

The activity of single neurons was recorded extracellularly. A 7-channel multielectrode recording system (Eckhorn System, Thomas Recording, Marburg, Germany) was used. In combination with 7 dual time–amplitude window discriminators (Bak Electronics Inc., Mount Airy, MD), recording could be obtained from up to 14 cells simultaneously. Electrodes were glass-coated tungsten–platinum fibers (1–2 MOhm impedance at 1 kHz). The eye coil, recording chamber, and head holder were implanted aseptically under general anesthesia (sodium pentobarbital, 25 mg/kg; intravenously).

Data Analysis

Analysis of Neuronal Activity

In each task, the average firing rate during different epochs was computed on a trial-by-trial basis. In any given epoch, significant modulation of neural activity relative to the CT or to the target direction was studied through a 2-way analysis of variance (ANOVA) (factor 1: epoch; factor 2: direction). The neural modulation relative to CT was assessed when factor 1 and/or the interaction factor 1 × 2 were significant ($P < 0.05$). The same kind of ANOVA was used to depict significant difference between 2 different epochs of 2 different tasks (factor 1 and/or factor 1 × factor 2, $P < 0.05$). The data were analyzed by using the program 5V of the BMDP statistical package (STATISTICAL Solutions, CA). For each cell, the epochs included in the ANOVA were such that the neural activity had to be different from 0 spikes/s in at least 3 replications, tested in at least one direction of movement. Thus, cells with 0 spikes/s in all directions and replications were excluded from the analysis. However, cells that had zero spikes in all replications in a given epoch because of suppression, but were active in adjacent temporal epochs, were included in the analysis because in such a case the absence of spikes did not depend on absence of task relationships. For this
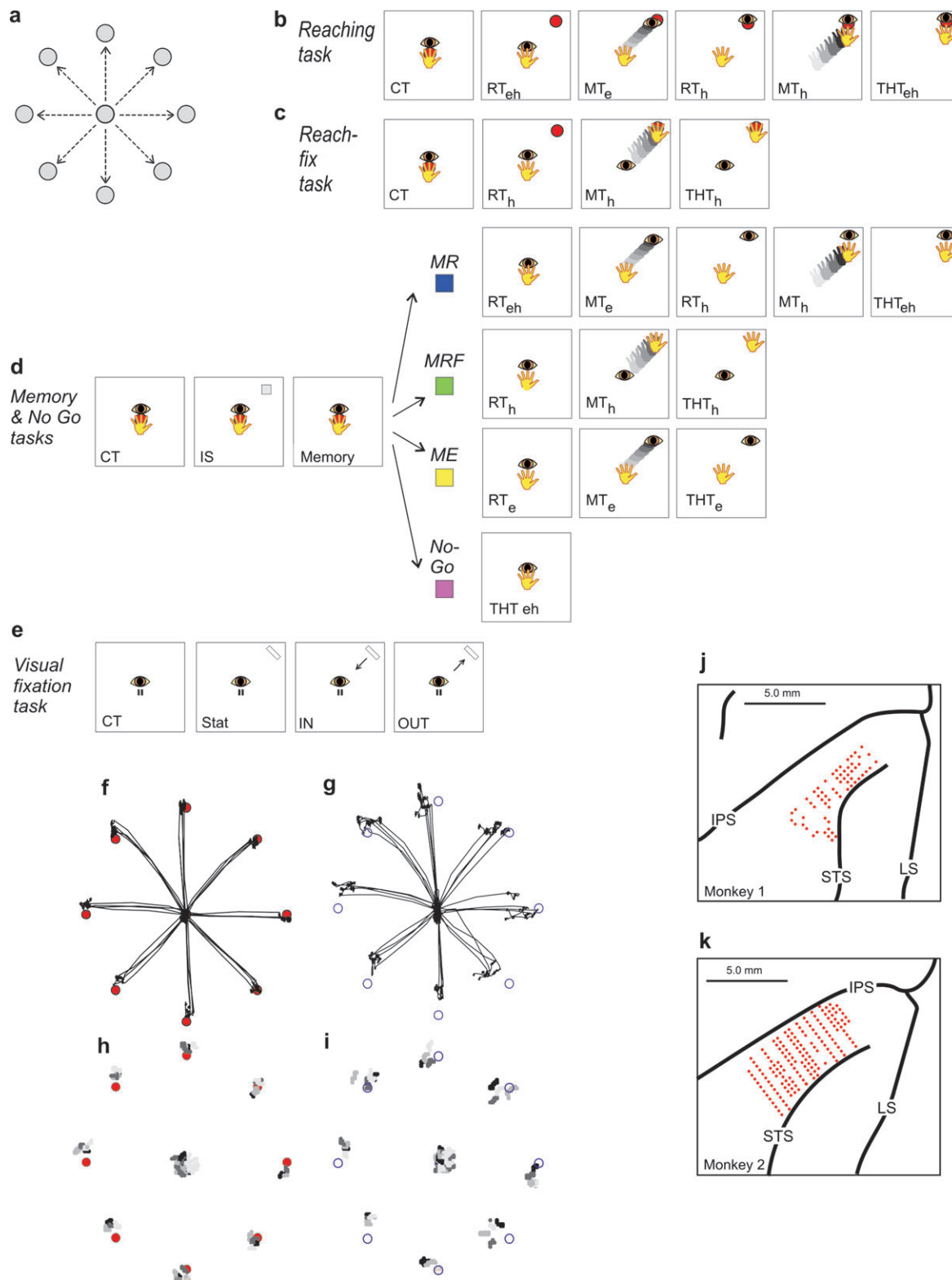
Figure 1. Behavioral tasks and performance and recording sites. (a) Directional layout of the workspace used for all tasks. Circles indicate central and peripheral targets. (b–e) Schematics of the temporal structure of the reaching, reach-fix, memory reach (MR), memory reach-fix (MRF), memory eye (ME), No-Go, and visual fixation tasks. In each task, the color of the IS is indicated by the corresponding small square; RTeh, eye–hand reaction time; RTh, hand reaction time; RTe, eye reaction time; MTe, eye movement time; THTe, eye target holding time; MTh, hand movement time; THTeh, coordinated eye–hand target holding time; THTh, hand target holding time; Stat, stationary presentation of the visual stimulus; IN and OUT indicate inward and outward motion of the visual stimulus, respectively. In (e), the 2 vertical bars at the center indicate the FP. Records of eye movements and of hand positions in the visual reaching (f–h) and in the memory reaching (g–i) tasks obtained in the same behavioral session. In (f) and (h), red circles indicate visual targets; in (g) and (i), the blue circles indicate the locations where the IS was presented. In (h) and (i), the 4 gray levels indicate 4 different replicas of the origin and end points of hand movement. (j–k) Recording sites in area 7a of 2 left hemispheres of 2 monkeys. Red dots indicate microelectrode penetrations. IPS, intraparietal sulcus; STS, superior temporal sulcus; LS, lunate sulcus.

reason, the total number of cases accounted to compute proportion of cells can vary across epochs within the same task. The temporal span of analysis of some epochs was adjusted: the first 500 ms of CT were excluded from analysis to prevent potential effects of previous eye and/ or hand movement; the first 300 ms of the memory delay activity were removed to avoid influences of visual responses to the IS; and finally, the first 300 ms and the last 500 ms of THT were not considered, to avoid influence of previous movements or planning of return movements to the center during the intertrial interval.

Index of Modulation of Neural Activity

To quantify the relative strength of the signals influencing neural activity in representative task epochs, a modulation index M_{ni}, associated to each cell n and epoch i, was computed as follows:

$$M_{ni} = \frac{f_{ni} - f_{nc}}{f_{nc}}, \qquad (1)$$

where f_{ni} is the mean frequency across repetitions and directions of the cell n during epoch i, and f_{nc} is the mean frequency of the same cell during the CT. The indices derived from different epochs were used to compare the proportion of cells influenced by different eye and/or hand signals across tasks. The differences among distributions were evaluated by computing their median values. The Spearman rank correlation analysis was used to compare the median values of the modulation indices between different behavioral conditions.

The modulation indices of different signals were obtained by analyzing neural activity during certain epochs of any given task, as follows:

1. memory eye: memory delay epoch of memory eye task,
2. memory hand: memory delay epoch of memory reach-fix task,
3. memory eye–hand: memory delay epoch of memory reach task,
4. No-Go: delay epoch in the No-Go task,
5. eye movement: eye MT in memory eye task,
6. hand movement: hand MT in memory reach-fix task,
7. eye position: THT in memory eye task,
8. hand position: THT in memory reach-fix task,
9. eye–hand position: THT in memory reach task,
10. hand movement to FP: hand MT in memory reach task,
11. visual IS: 300 ms of IS in memory eye, memory reach, memory reach-fix, No-Go tasks.

Visual Receptive Fields

Color-coded maps of the visual receptive field of individual neurons were generated from data collected during the "visual fixation" task. For each trial, the arrays of neuronal spikes were divided into 16 bins located along the movement trajectory of the visual stimulus, at even intervals, with each bin representing a specific area of the visual field. Any given spike was allocated to a specific bin, based upon the trial and the time of spike occurrence. This assumes that any activity of the cell is due to the presence of the visual stimulus. To derive the cell's firing frequency in any particular part of the visual field, the number of spikes in each bin was then divided by the time the visual stimulus stayed in that bin. The cell activity in each discrete area of the visual field was normalized by averaging the activity of the 3 closest bins.

Analysis of Onset Times (OTs) and of Temporal Profiles of Cell Activity

The OTs of activity increase were computed relative to eye movement and hand movement. A spike density function (SDF) was calculated for each cell, using a Gaussian kernel with half width (standard) of 40 ms. SDFs were aligned to the behavioral event of interest and then averaged across all the available repetitions in each direction. For each cell and task epoch, a preferred direction was determined as the stimulus or movement direction that elicited the highest average firing rate. The SDF for this direction was the only one considered for both population grand averages and OT of cell activity. OT of neural activity was computed using an algorithm (Richmond and others 1990) based on sliding windows of 80 ms. Population statistics of OTs in different behavioral epochs were performed only on those cells with activity significantly (ANOVA, $P < 0.05$) different in the 500 ms before and after the event used as alignment.

To compute the OT of the neural activity in different tasks, we have first aligned the activity to a common event that was identical in all the tasks compared. This choice has the advantage to use a common criterion that is task independent and not biased by the event chosen as alignment. For the memory tasks, we have used as common alignment the Go signal, which in all instances coincided with the off of the central light, whereas for the visual reaching tasks, we have adopted the presentation of the peripheral target, which in such instances also serves as Go signal. However, in order to understand the meaning of the OTs of cell activity obtained with this common alignment (i.e., to see if OTs leaded, coincided, or followed movement), we have rescaled them with respect to the different forms of behavior that distinguished the different tasks. To this purpose, for each cell, the value of the OT of activity was subtracted from the time the eyes start to move (memory eye task) or from the time the hand starts to move (memory reach, memory reach-fix, reaching, and reach-fix tasks), so that the zero of the new temporal scale now corresponds to the beginning of eye or hand movement. This realignment of OTs offers a better picture of the nature of the neural response. The same cells used to compute OTs were also used to compute the population SDFs. These were obtained by averaging all the density functions of the cells aligned on a given behavioral event, for the particular task of interest.

At individual cell level, the difference in the time of occurrence of the peaks of neural activity observed in different tasks was computed. This analysis was performed on those cells that combined eye and hand information ("eye–hand cells," see below) and that therefore displayed 3 prominent activation peaks once aligned to the Go signal. The first peak was in the memory eye, the second in the memory reaching, and the third in memory reach-fix tasks. For these cells, the maximum temporal difference among peaks was plotted in the form of frequency distribution.

The analysis of the relationships between OT of neural activity and task events was also applied to data available from previous experiments on areas PEc and V6A, where neural activity had been studied during a reaching, a reach-fix, and a "saccade" task. Details on these tasks are given in Battaglia-Mayer and others (2000, 2001).

Functional Cell Types

To assess eye and/or hand dominance on neural activity, all cells significantly modulated in all 3 memory tasks were used as database. A super-preferred direction was computed as the stimulus direction that elicited the highest cell activity in the 1-s period following the Go signal, across the memory eye and memory reach-fix tasks. Eye-dominant cells were defined as those for which neural activity at the super-preferred direction was significantly (1 tail Z-Test, $P < 0.05$) higher in the memory eye than in the memory reach-fix task. In the memory eye task, to guarantee for the presence of a significant activation at the Go signal, cell activity in the time window chosen also had to be modulated with respect to the previous 0.5 s. Hand-dominant cells were determined in the same fashion, by requiring activity in the memory reach-fix task to be significantly higher than that in the memory eye task. Among those cells that did not fit the above categories, eye–hand cells were defined as those for which neural activity was significantly higher in the 1-s interval following the Go signal (relative to the 0.5 s before it) of the memory eye, memory reach, and memory reach-fix tasks.

Results

Recording Sites

The activity of 559 individual neurons was recorded in area 7a of 2 left hemispheres of 2 monkeys while the 7 different tasks were performed (Fig. 1a–e). In both monkeys (Fig. 1j,k), microelectrode penetrations were made in a region of the IPL that has been identified as area 7a, on the basis of 2 main criteria: 1) the histological reconstructions of the microelectrode tracks relative to gross anatomical landmarks, such as the position of the intraparietal and superior temporal sulci and 2) the architectonic features of the area of recording. In both animals, penetrations were oriented perpendicularly to the cortical

surface, and the extent of recording was usually confined within 2 mm from the top of neural activity, with an average depth across all penetrations of 853 ± 25 μm (standard error) from top of neural activity. This indicates that the results obtained in this study refer to the flat exposed part of IPL. The details about the recording sites have been previously reported in Battaglia-Mayer and others (2005).

Co-occurrence of Visuospatial, Eye, and Hand Signals

A standard analysis based on the quantitative evaluation of cells modulated (ANOVA, $P < 0.05$; see Materials and Methods) across the different tasks and epochs revealed that visuospatial, eye, hand, as well as combined eye–hand signals influenced neural activity in the majority of the neurons studied. Modulation of neural activity occurred after the presentation of the IS,

during the memory delay, at the time of planning and execution of movement, and during static eye and/or hand holding on visual targets or memorized locations (see Supplementary Materials for details). Noticeably, the highest cell recruitment was observed during 1) active holding of eye (memory eye) on memorized locations; 2) hand movement toward the FP (memory reach and reach); and 3) hand movement to visual targets and away from the FP (reach-fix). Across the temporal evolution of the tasks, different cells were preferentially activated in different epochs, from the onset of the visual instruction to the end of movement. Therefore, the overall performance of the visuomotor tasks resulted in a graded recruitment of parietal cells.

Figure 2 illustrates the results obtained from an individual cell studied in the 7 tasks adopted. The activity of this cell was
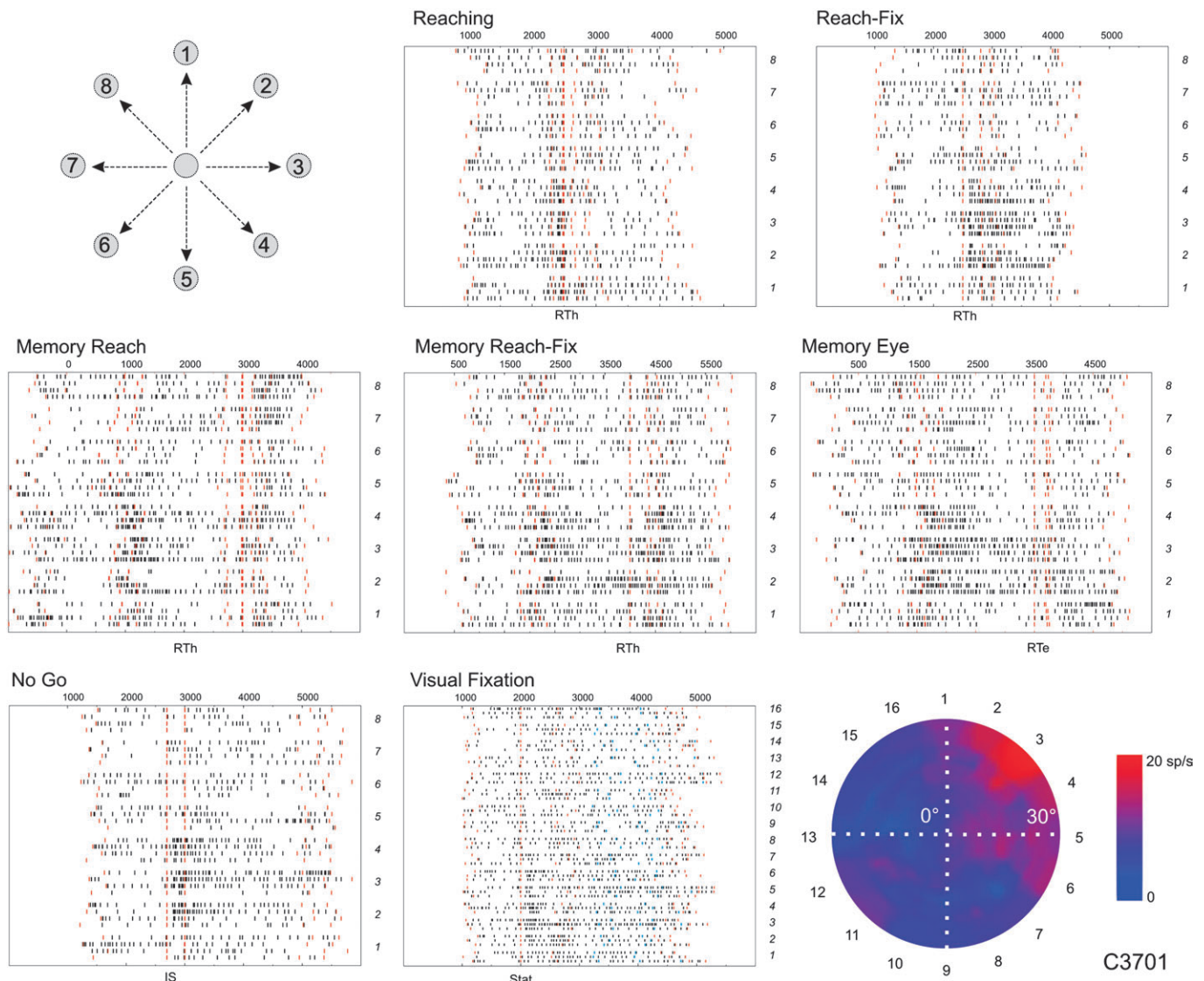

Figure 2. Neural activity of a parietal cell studied across the 7 behavioral tasks of this study. The layout of the workspace for the eye and hand tasks is schematized in the left upper part of the figure. In each panel, rasters of 4 replications of neural activity in 8 directions of movement, or 16 directions of visual stimulations, are aligned (vertical red line) to different behavioral events. Small black vertical lines indicate the occurrence of an action potential, each sequences of red vertical lines separate behavioral epochs. In the visual fixation task, rasters are aligned to the onset (Stat) of stationary presentation of the visual stimulus, whereas blue lines indicate the moment of change of direction of stimulus motion. The color contour maps of the visual field shows the visual response area of this cell, as computed from neural activity illustrated in the raster display of the visual fixation task. In the color contour maps, 0° corresponds to the fovea. Horizontal and vertical meridians of the visual field are shown by white dotted lines, the numbers indicate the direction of stimulus motion. The color calibration bar is in spikes/s. RTh, hand reaction time; RTe, eye reaction-time; IS, presentation of the instruction signal; Stat, presentation of stationary visual stimulus.

significantly modulated in a direction-selective fashion across several task epochs related to different information, such as hand movement and position (reach-fix, memory reach-fix), eye position (memory eye), combined eye–hand position (memory reach), and memory delay (memory reach-fix, memory reach, memory eye, No-Go), by the visual stimulation occurring after presentation of the ISs (memory reach-fix, memory reach, memory eye, No-Go), after visual target presentation (reach and reach-fix), as well as after presentation of stationary visual stimuli in the visual fixation task.

Despite the fact that in most instances each cell was modulated by a variety of different eye–hand information, parietal cells could be characterized by the predominant influence of a given signal on neural activity. In fact, 376/559 (67%) cells were modulated in all the 3 memory tasks and therefore can be considered as "combinatorial cells." By using the quantitative criteria illustrated in Materials and Methods (see Functional Cell Types), 3 main classes of combinatorial neurons have been identified among those studied during the memory tasks, where no visual information was available to the monkey during eye and/or hand movement. Figure 3 shows the neural activity in the form of rasters and SDFs across 3 different memory tasks, for 3 different cells, each representative of a main functional type. In Figure 3a, a cell is shown whose activity was dominated by hand movement, therefore labeled as "hand-dominant cell." Neural firing mostly occurred during hand movement (blue line), with little modulation during eye movement (green line). When the hand moved shortly after the eye toward a memorized target location, that is, to the current FP, an intermediate strength of modulation was observed (red line). An "eye-dominant cell" is presented in Figure 3b, with neural activity strongly modulated during eye movement (green line) and poorly modulated by hand movement (blue line). Significant modulation was also observed during hand movement to the current FP (red line). Figure 3c shows the activity of an eye–hand cell, where eye alone (green line), hand alone (blue line), and combined eye–hand movement (red line) contribute similarly to the cell's firing rate. At the population level, among the combinatorial cells, eye-dominant cells were 125/376 (33.2%), hand dominant were 36/376 (9.6%), and eye–hand cells were 127/376 (33.8%). It is worth noticing that these cells could also be sensitive to visual stimuli.

This categorization, based on data from the memory tasks, leaves open the possibility that the combinatorial parietal cells just described were also influenced by visual information. Out of the combinatorial cells that were also studied in the visual fixation task, the activity of 79/89 (88.8%) eye dominant, 20/23 (86.9%) hand dominant, and 81/96 (84.4%) eye–hand cells was significantly modulated (ANOVA, $P < 0.05$) by visual stimulation. Therefore, the largest majority of combinatorial cells were also visual in nature.

Visual Responsiveness

Individual neurons in area 7a had visual response areas that were generally very large and mostly located in the periphery of the visual field (Fig. 4b). A significant proportion of cells were modulated by the stationary presentation and movement of visual stimuli while the animal fixated a center light. Stationary visual stimuli influenced the activity of 354/489 (72.3%) cells tested (Fig. 4a). The cells modulated by visual stimuli moving IN toward the fovea (Fig. 4a,b) were 220/489 (44.9%), whereas 265/489 (54.1%) cells responded to stimuli moving OUT, from the fovea to the periphery of the visual field. The cells significantly modulated by both IN and OUT components of stimulus motion were 162/489 (33.0%). Considering that, among these only 17/162 (10.4%) cells did not show a significant difference of activity between the 2 directions, it can be concluded that most cells (306/489, 62.5%) of the population were selective for the direction of stimulus motion. In fact, 58/489 cells were selective only to IN motion, 103/489 to OUT only, and 145/489 responded to both IN and OUT motions of the visual stimulus, although with significant differences between the 2. These properties are reminiscent of those of visual parietal cells, as first described by Motter and Mountcastle (1981), although we have not explored in detail the opponent vector organization for cells with bilateral response fields.

Parietal visual cells, as determined in the visual fixation task, were also active during arm reaching. In particular, those active during RT and movement time of the memory reach and memory reach-fix tasks, therefore in absence of any visual stimulation, were 192/371 (51.7%) and 183/376 (48.7%), respectively. Those active during the same epochs of the reaching and reach-fix tasks, when reaches were made to visual targets, were 210/390 (53.8%) and 208/384 (54.2%), respectively.

Strength of Neural Signals

The strength of different signals influencing neuronal activity in area 7a has been evaluated through the modulation index
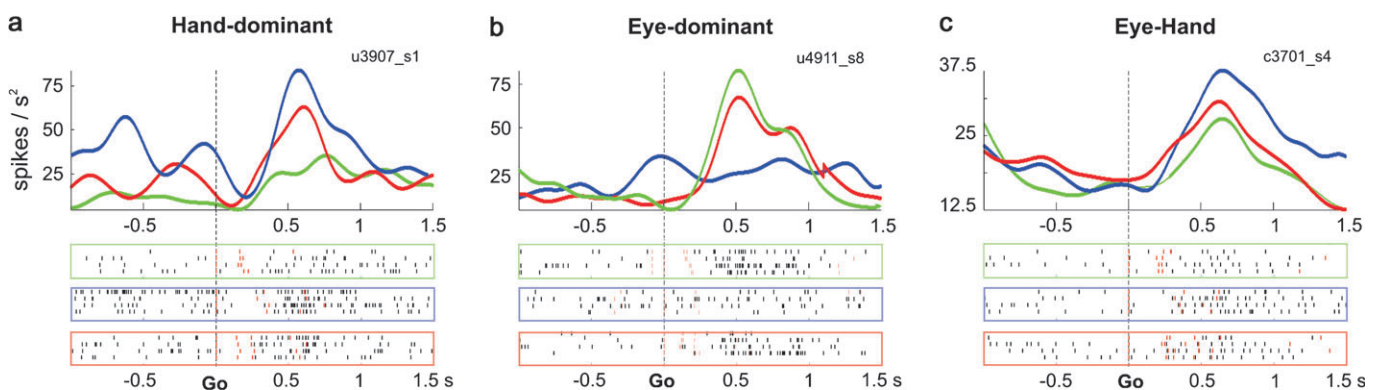
Figure 3. Combinatorial cell types in area 7a. SDFs (color curves) and raster displays of neural activity at the super-preferred direction for 3 different cells, each studied in the memory eye (green), memory reach-fix (blue), and memory reach (red) tasks. Different behavioral epochs are delimited by red vertical lines. Rasters and SDFs are aligned to the Go signal (vertical interrupted line).
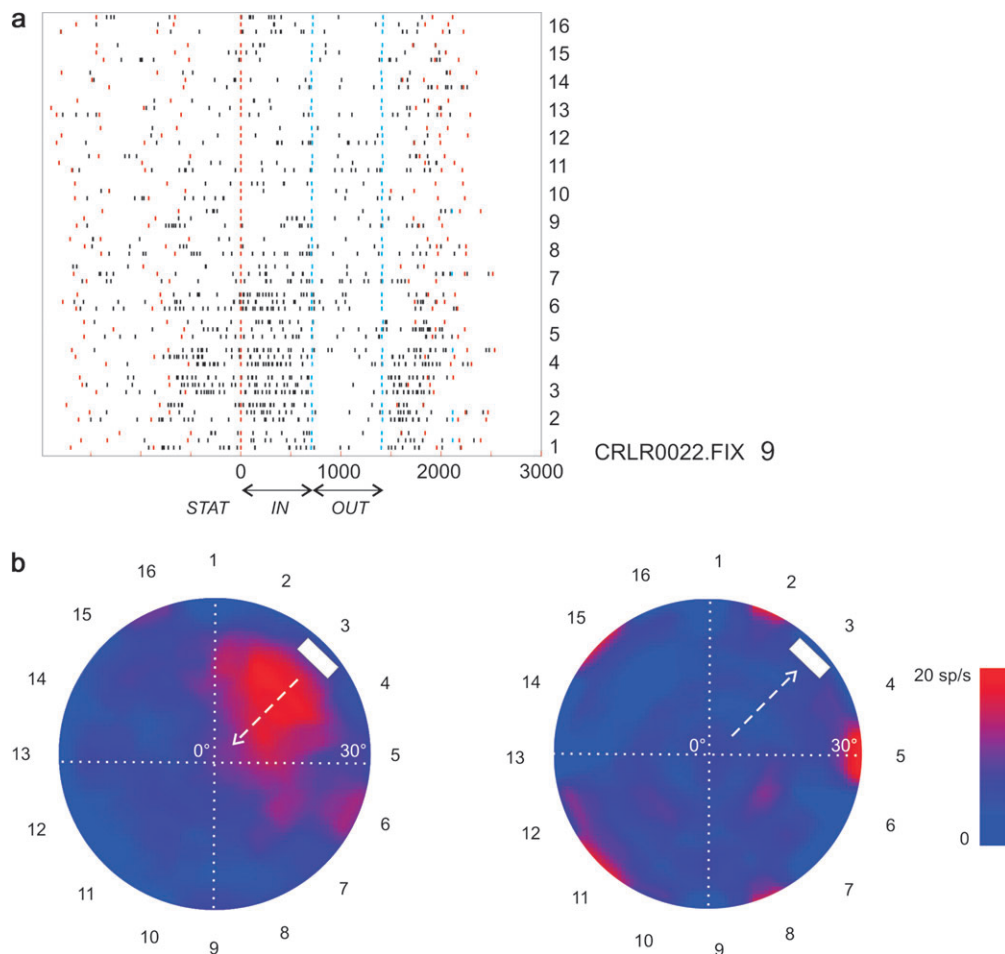
Figure 4. Visual properties of neurons in area 7a. (*a*) Raster display of cell activity of an individual neuron in the visual fixation task, during static presentation (STAT) and movement of a visual stimulus (solid white rectangle) along 16 different directions, IN and OUT, relative to the fovea (FP). Rasters are aligned to onset of IN movement of the stimulus. Red lines separate behavioral epochs and blue lines indicate the moment of change of direction of stimulus motion. (*b*) Visual response of the same neuron shown in (*a*) in the form of color contour maps, for selective IN (left) and OUT (right) stimulation. Note the contralateral visual response area for IN motion only. Other conventions and symbols as in Figure 2.

M, as detailed in Materials and Methods. Different values of *M* relative to individual signals (i.e., eye position, hand position, etc.) or to a combination of some of them (i.e., eye position + hand movement, etc.) were computed. The comparison of the median values of *M* across task epochs (Fig. 5) shows that these signals influenced the cell population studied with different strength.

Visual IS and Memory Delay
In the memory reach, memory reach-fix, and memory eye tasks, the IS was cue for future coordinated eye–hand movement (MR), hand movement (MRF), or eye movement (ME). The median value of *M* was similar across these task conditions and at all instances higher than that observed in the No-Go and in the visual fixation task, where the visual stimulus did not call for any future movement. In the memory epochs, the median value of *M* was among the weakest seen across all task periods studied.

Reaction Time
Parietal cell modulation during this preparatory epoch was very weak across all task conditions. Modest activity was only observed during preparation for hand movement toward the FP (MR).

Eye Movement
Eye movement was much more effective in modulating cell activity when made in the context of a coordinated eye–hand movement to visual targets (R), rather than to memorized locations (MR). Activity during isolated saccades to memorized location (ME) had little effects on cell firing rate.

Hand Movement
During hand movement, significant modulation was obtained, in decreasing order of magnitude, during reaches to the fixation point in absence (*MR*) or presence (*R*) of visual targets, and during reaches to memorized locations, in absence of eye movement (*MRF*). The modulation associated to hand movement toward the fixation point was the highest observed across all task epochs studied.

Eye and/or Hand Position
The strongest signal observed in this class was that related to eye position (ME), whereas the signal concerning hand position and combined eye/hand position was very weak, suggesting a strong nonlinearity in the interaction between eye and hand position information across task.

Temporal Relationship between Neural Activity and Behavior

The OT of the neural activity was studied relative to the beginning of eye and of hand movement. In the latter case, the analysis was performed when movement was performed with and without preceding saccades. In the memory eye task (Fig. 6a), the majority of cells fired after the beginning of eye movement, thus confirming their postsaccadic nature (Barash and others 1991), whereas a smaller but substantial number of them fired before and during the saccade. On the contrary, more than half of the cells studied began to fire before hand movement, when this occurred with (Fig. 6b) or without (Fig. 6c) prior eye movement to memorized targets.

Figure 7 shows the population SDFs observed during different memory tasks (memory eye, green; memory reach, red; memory reach-fix, blue), and in the No-Go task (yellow), aligned to the IS (Fig. 7a) or Go signal (Fig. 7b). After presentation of the IS (Fig. 7a), the 4 population activities showed similar temporal evolutions, revealing a brisk response to the visual stimulus (shaded area) with a maximum at 173 ± 17 ms (visuospatial peak) and a local minimum at the off of the visual cue (300 ms

after IS presentation). In Figure 7b, the population activity relative to the 3 memory tasks changed early after the Go signal, evolved, and peaked (motor peak) in a similar fashion at 455, 444, and 451 ms after the presentation of the Go signal. These maxima of activity are very close to each other, in spite of the fact that the behavioral events following the Go signal were totally different across the 3 tasks. The average values of behavioral data obtained from the same animals show a buildup of population activity occurring mostly after the end of eye movement but before and during hand movement. As far as these specific signals are concerned, their relative strength seems to reflect that observed through the task epoch analysis, the strongest population signal being the one relative to coordinated eye–hand movement. Strikingly, virtually no population activity (Fig. 7b, yellow) was elicited when the cue signal instructed the animal to keep the eye and the hand on the central position of the workspace and not to go.

As confirmation of the previous analysis, we investigated whether or not the alignment in the peaks of neural activity seen at the population level after the Go signal for movement could also be observed at the single-cell level. For this analysis,
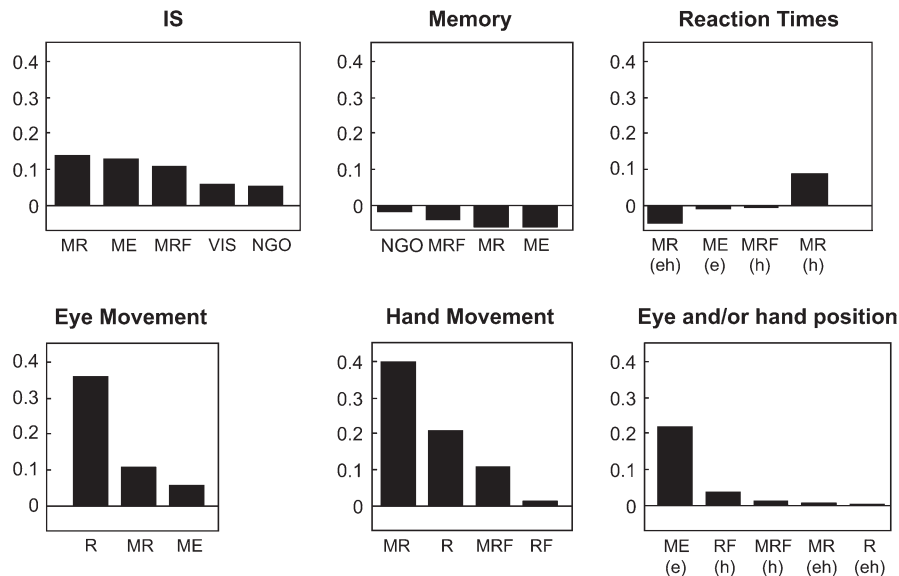

Figure 5. Modulation indices. Distributions of the median values of the modulation indices for the entire population of cells studied in different epochs across tasks.
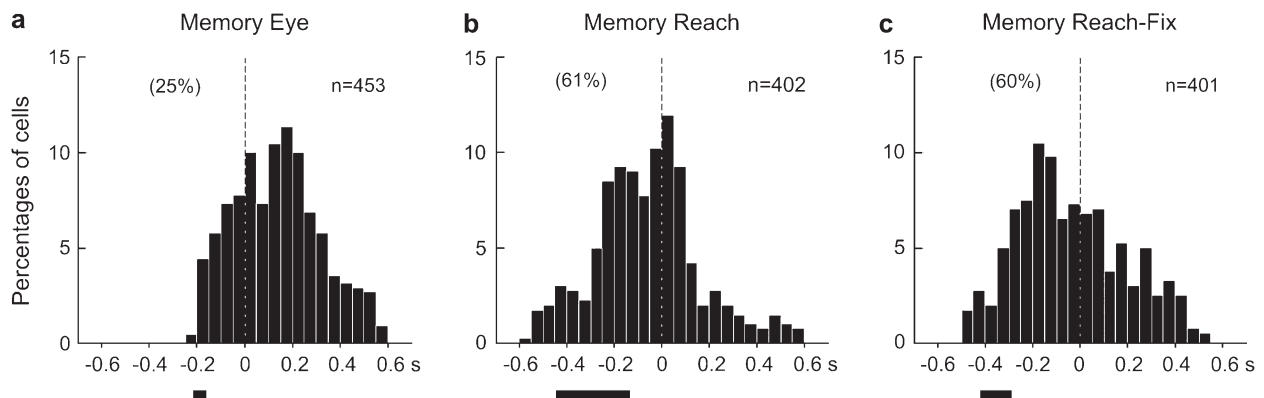

Figure 6. OTs of neural activity in the memory tasks. Frequency distributions of OT of cell activity relative to eye movement only (a), coordinated eye–hand movement (b), and hand movement (c) only. Vertical interrupted lines indicate the beginning of movement. Percent in brackets indicate the proportion of cells firing before movement onset. Thick horizontal bars below the x axes refer to begin of RT ± standard deviation.
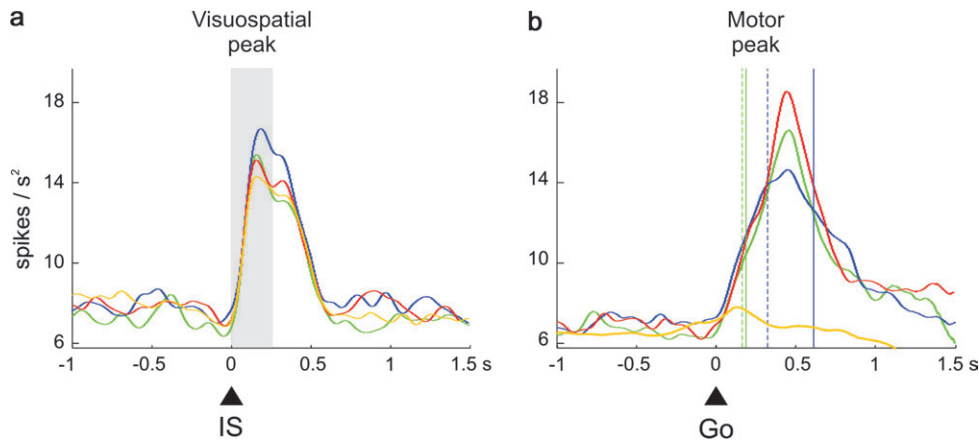
Figure 7. Population activities in the memory tasks. Population SDFs aligned to the IS (*a*) and Go signal (*b*). memory eye (green), memory reach (red), memory reach-fix (blue), No-Go (yellow). In (*a*), the gray vertical shading indicates the duration of the IS. In (*b*), vertical lines indicate from left to right median values of beginning of eye MT (164 ms, interrupted green), end of eye MT (188 ms, solid green), OT of hand movement (324 ms, interrupted blue), and end of hand MT (613 ms, solid blue). Therefore, the 2 green lines encompass the median value of the duration of eye MT, whereas the 2 blue lines the median value of the duration of hand MT.

we selected those cells (eye–hand) that displayed 3 prominent activation peaks, one relative to combined eye–hand action, the second to eye movement, and the third to hand movement. Figure 8 shows that for most cells, the maximum temporal spread in the occurrence of the 3 peaks was rather limited and below 50 ms.

The relationships between the timing of cell activity and behavioral events were also studied during the reaching and reach-fix tasks. For this analysis, we have also used, for comparative purposes, data available from previous experiments (Battaglia-Mayer and others 2000, 2001) where cell activity had been recorded in the parieto-occipital cortex (SPL, areas PEc and V6A) during identical tasks, as well as in a saccade task, where monkeys made saccadic eye movement in different directions to visual targets within a RT paradigm.

In area 7a, during reaches to foveated targets (Fig. 9*a*, reaching), 30% of the cells studied apparently started to fire before hand movement; on the contrary, 59% of them did so during reaches to extrafoveal targets (Fig. 9*b*, reach-fix). It must be stressed that the length of the hand RT was significantly shorter in the reaching than in the reach-fix task (Fig. 9*a–b*).

In both cases, the peak of both distributions occurred about 120 ms after the beginning of RT, which by definition coincides with visual target presentation. This suggests that the shape of these distributions is, at least in part, determined by visual inputs.

In SPL, most (about 70%) cells studied fired well before the onset of hand movement in both tasks (Fig. 9*c,d*). The temporal evolution of the population activity (Fig. 10) was virtually identical during reaches to foveated and extrafoveal targets, displaying a single peak at 235 ms after target presentation (Go signal), followed by a slower decaying phase lasting about 800 ms. A very similar evolution and peak of the activity profile was obtained during eye movement to visual targets.

In area 7a (Fig. 10), when reaches were made to foveated targets, cell activity increased after target onset and displayed 2 peaks, a smaller one at 161 ms and a larger one at 387 ms after target presentation. During reaching to extrafoveal targets, the difference in amplitude between the 2 peaks was less evident; however, their temporal occurrence roughly coincided with that of the reaching task. We then compared the temporal
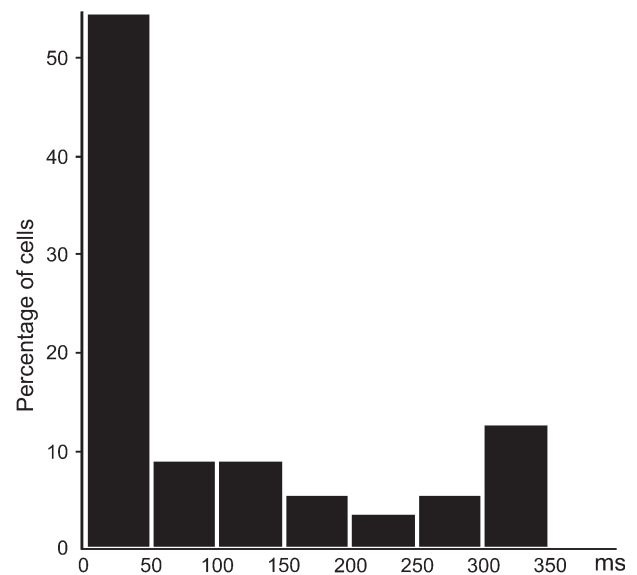

Figure 8. Temporal spread of the activity peaks of eye–hand cells in the memory tasks. Frequency distribution of the maximum temporal difference among the peaks of neural activity observed at single-cell level, after the Go signal in the memory eye, memory reach, and memory reach-fix tasks.

evolution of the population activities obtained in these RT tasks with those observed in the memory tasks and found that for both RT tasks the first peak aligns to the visuospatial peak, whereas the second one coincides with the motor peak of the memory tasks. This is better shown in Figure 11, where the population activities obtained from the 3 memory tasks (gray) and from the reaching (red) and reach-fix (blue) tasks are aligned to the IS and to the Go signal. These alignments of data from different tasks were possible because the visual target presentation of the visual reaching tasks not only was similar to the presentation of the visual IS of the memory reaching tasks but also served as Go signal. In all instances, the population maxima were greater in SPL than in IPL, and the time of occurrence of the motor peak was earlier in the former (235 ms) than in the latter (387 ms).
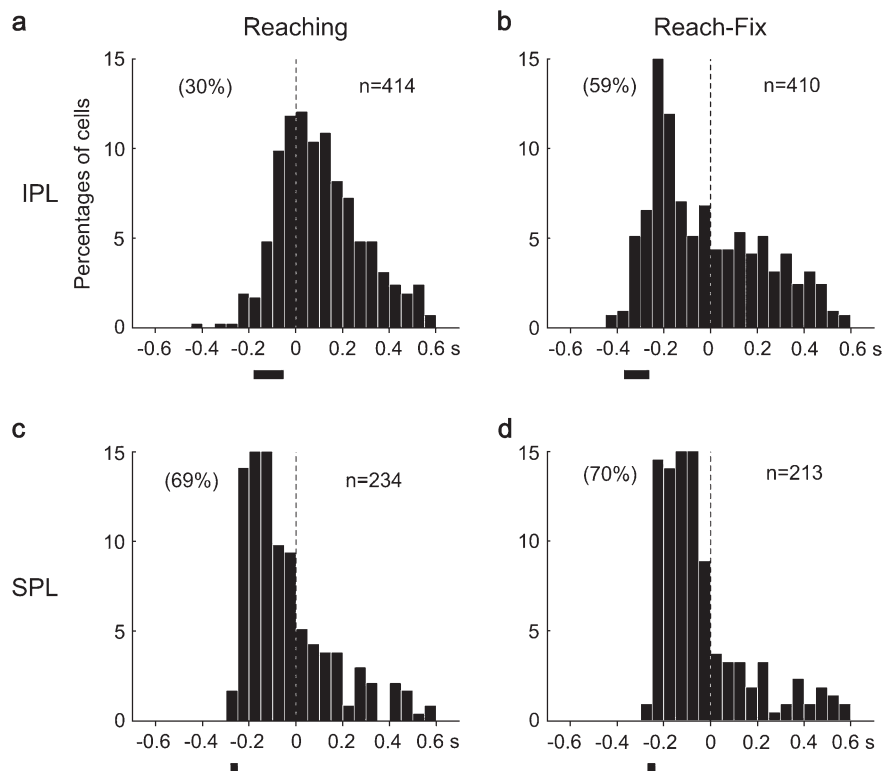
Figure 9. OTs of neural activity in the visual reaching tasks. Frequency distributions of OT of cell activity relative to hand movement to visual targets with (reaching) and without (reach-fix) prior eye movement. (a, b) Data from area 7a, in the IPL. (c, d) Comparative data from areas V6A and PEc, in the SPL. Vertical interrupted lines indicate the beginning of hand movement. Percent in brackets indicate the proportion of cells firing before the onset of hand movement. Thick horizontal bars below the x axes refer to begin of RT ± standard deviation.

Discussion

This study indicates that the activity of the majority of neurons studied in area 7a combined retinal, eye, and hand information. A large proportion of them responded to the presentation of conventional visual stimuli and had large, often binocular, receptive fields. Both stationary and moving stimuli elicited vigorous responses. A large fraction of cells displayed direction specificity, whereas a substantial number of them were sensitive to the direction of stimulus motion. These properties conform to what already described in previous studies of parietal cortex (Mountcastle and others 1975, 1981; Lynch and others 1977; Robinson and others 1978; Motter and Mountcastle 1981).

Neurons in area 7a not only responded to visual stimuli but also and more vigorously to the visual cue signal that instructed the animal about a future movement. In fact, both the proportion of cells recruited and their responses to the visual stimulus were higher in the memory tasks, when the visual cue called for a future movement, than in the visual fixation or in the No-Go task, where the animal was, respectively, required to fixate or instructed not to move the eye and/or the hand. This indicates an enhancement of visual responses by behavioral events (Robinson and others 1978; Bushnell and others 1981; Mountcastle and others 1981).

The activity of about half of the parietal visual cells studied was also modulated during hand movement, and this proportion did not change significantly depending on whether movement was directed to a visual target or to a memorized location. This suggests that the relationship between cell activity and hand movement in area 7a is independent from the visual properties of neurons.
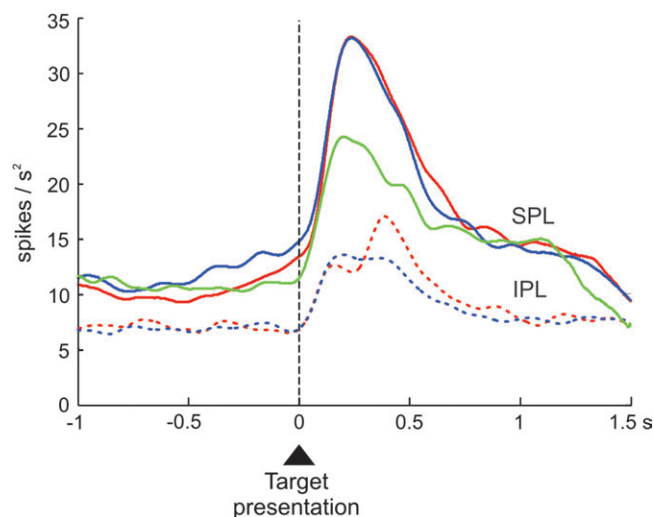

Figure 10. Population activities during hand movement and eye movement to visual targets. Population SDFs aligned to the presentation of the visual target in the reach (red), reach-fix (blue), and saccade (green) tasks. SPL data (areas PEc, V6A), solid lines; IPL (area 7a), interrupted lines.

Coexistence of eye and hand signals was observed in all epochs across task conditions, such as memory delay, RT, movement time, and static holding on peripheral targets, both in the presence and absence of visual stimuli in the experimental scenario. It can be concluded that, under the experimental conditions of this study, neural activity in area 7a is influenced by visuospatial signals about target location, by planning and
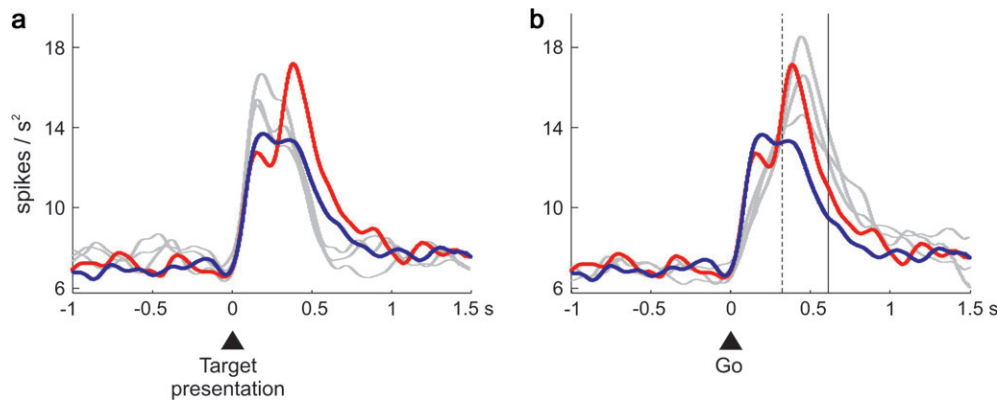
Figure 11. Population activities in area 7a, across different task epochs and conditions. In (*a, b*), the gray population SDFs are those obtained in response to the presentation of the visual IS or Go signal (Go) in the 3 memory and the No-Go tasks (see Fig. 7 *a,b*), whereas the red and blue population SDFs are those obtained after visual target presentation in the reaching (red) and reach-fix (blue) tasks. In (*a*), notice the alignment of the first (visuospatial) peak of the population activities in the reaching (red) and reach-fix (blue) tasks with the visuospatial peaks (gray) of the population activities in the memory and No-Go tasks. In (*b*) is shown the alignment of the second (motor) peak of the population activities in the reach (red) and reach-fix (blue) tasks with the motor peaks (gray) of the population activities obtained after the Go signal for movement in the memory and No-Go tasks. Vertical black lines indicate the OT of hand movement (324 ms, dashed) and end of hand MT (613 ms, solid blue).

execution of coordinated eye–hand movements, as well as by information on eye and/or hand position in space.

Based on the relative strength of hand and eye influences on neural activity, we have tentatively identified 3 main classes of combinatorial cells in area 7a: eye dominant, whose activity was dominated by eye signals; hand dominant, mainly influenced by hand signals, eye-hand, where neural activity was influenced with similar strength by eye and hand information. This classification does not depend on the visual properties of neurons because it was derived from cell activity studied in the memory tasks, where movement was performed in absence of visual signals, although most combinatorial reach cells were also sensitive to visual stimuli. It is possible that these 3 populations of cells result from the convergence of weighted eye and hand inputs into 7a cells. In this study, recording was mostly performed in that part of area 7a that, according to Pandya and Seltzer (1982) and Rozzi and others (2005), is labeled as Opt. The long corticocortical connections with the agranular frontal cortex, the intraparietal connections with SPL areas known to combine eye and hand signals, such as 7m (Ferraina, Garasto, and others 1997; Ferraina, Johnson, and others 1997) and V6A (Battaglia-Mayer and others 2000, 2001), as well as the short and dense local connections with area PG (Rozzi and others 2005) can very well explain the converge of visual, eye, and hand information on individual cells in area Opt.

Earlier studies of reaching in the IPL (Hyvärinen and Poranen 1974; Mountcastle and others 1975; Blum 1985; MacKay 1992) did not evaluate the relative influence of retinal, eye, and hand signals on neural activity. Only Snyder and others (1997) described the preponderance of activity types, reflecting the intention to perform eye versus hand movements in IPL. The proportion of cells combining eye–hand signals, referred to as "nonspecific," was reported to be small. Calton and others (2002) described hand movement–specific cells in a subregion of parietal cortex that should correspond to a portion of area 7a. In these studies, the precise identification of the recording sites and their attribution to specific cortical areas is not available. The results of our study show that the majority of cells in 7a are influenced by combined eye-hand information. This discrepancy might be explained by considering that the 2 above-mentioned studies drew their conclusions from cell activity

studied only in the memory epochs across 2 conditions, whereas in our experiment, the co-occurrence of eye-hand influences was assessed across a multiplicity of behavioral task epochs.

Memory-related activity was the weakest signal we were able to identify in area 7a (see also Constantinidis and Steinmetz 1996), in spite of the cognitive demands inherent to this task epoch. In fact, the 3 memory epochs of this study requested the identification of the color of the visual cue, keeping in the buffer of the working memory its spatial location, and the selection of eye, hand, or combined eye-hand movements. On the contrary, after the Go signal for movement, a brisk increase in neural activity was observed during RT and movement time, both at single cell and at the population level, and in absence of sensory target stimuli for movement.

Altogether, these results support the contention that cell activity observed during these epochs reflects a planning mechanism for coordinated eye and hand actions, as well as corollary signals of motor plans. Neural activity bound to eye or hand movement had already been described in different areas of both SPL and IPL (Mountcastle and others 1975; Lacquaniti and others 1995; Mountcastle 1995; Snyder and others 1997; Calton and others 2002).

The different signals described above influenced cell activity with different strength. In decreasing order of magnitude, they were eye position, hand movement, and eye movement. Thus, it is not surprising that the highest modulation across tasks was observed during hand movement time in the memory reach task, in other words, when the hand moved to the FP, therefore, to where the animal was attending at that particular instant. Thus, although eye position influence on neural activity during reaching can be instrumental to the process of visuomotor transformations necessary to encode target location in eye coordinates (Andersen 1995), in the behavioral context of our task, this information also reflects the active holding of the eye on a salient part of space, the one where the cue target signal was presented and, therefore, where selective attention was allocated (Lynch and others 1977; Robinson and others 1978; Bushnell and others 1981; Mountcastle and others 1981). Overall, this suggests that area 7a contains a neural code for coordinated eye-hand actions, based on selective spatial attention, necessary to position and keep the eye on salient targets

(Gottlieb and others 1998; Constantinidis and Steinmetz 2001, 2005), and motor planning to move the eye and the hand toward them. Corollary signals might be instrumental, during and at the end of movement, to maintain the spatial congruence between the eye and the hand. This mechanism can provide a population signal concerning the relevance of eye versus hand movement under different contexts, possibly by weighting the level of activity across the population of combinatorial reach cells. It can also be a source of input signals necessary to encode the position and movement of the hand relative to the FP. Combination of eye and hand signals is a process common to different parietal areas and can be the basis for that cascade of coordinate transformation from allocentric (Battaglia-Mayer and others 2000, 2001) to eye-centered (Batista and others 1999), body-centered (Lacquaniti and others 1995), and hand-centered (Averbeck 2005) coordinates described in parietal cortex under different task conditions.

This interpretation is also supported by the analysis of the temporal relationships between OT of neural activity and motor behavior. In fact, neural activities leading movement onset can be interpreted as part of a command, or motor planning mechanism, whereas those occurring around and after movement onset could reflect corollary signals of motor plans composed elsewhere in the brain, as well as the sensory feedback from the motor periphery. Our results show that in area 7a, about 75% of cells fired after the beginning of a saccade, as already known (Barash and others 1991), whereas the remaining fired before and during eye movement. Thus, neural activity in 7a leads, occurs during or after a saccade. On the contrary, about 60% of the cells studied discharged well before the onset of hand movement. This was not known before. The lead of cell activity relative to hand movement onset was observed in all task conditions, that is, when the hand moved to a visual or to a memorized target and when reaches were performed in the presence or absence of prior eye movement. Altogether, these data show the crucial importance of information related to hand movement while confirming the prominence of eye position versus eye movement signals in area 7a (Andersen and others 1990).

An intriguing result emerged when the population activities from individual task epochs were compared and aligned to common behavioral events. In the memory tasks, the population activities elicited by the signal instructing the animal to make a future eye, hand, or coordinated eye–hand movement, or not to move, had very similar temporal evolution and peaks (visuospatial peak), thus stressing the relevance of visuospatial inputs about target location in area 7a. The temporal coincidence of the peaks of activation was also obtained when population activities relative to the memory tasks were aligned to the Go signal (motor peak), in spite of the fact that the actions involved different effectors, such as the eye, the hand, or the both. The temporal span of the mean eye RT and movement time leaded the motor peak, as predicted by the postsaccadic activity observed in most cells. As far as the hand is concerned, the peak in the population activity coincided with movement onset, coherently with the premovement activity seen in a large fraction of parietal cell. In the No-Go task, when the animal was required to keep both the eye and the hand at the center of the workspace, the population activity elicited in area 7a was negligible. This temporal alignment of the peaks observed at the population level was also evident at single-cell level, as shown by the small variation in the time of occurrence of the activity peaks, when the cells were tested across different tasks.

The shape and temporal evolution of the population activity were also studied in the reaching and reach-fix tasks. It is worth remembering that in these tasks movement was made to visual targets within a RT paradigm. In area 7a, the shape of the population activity displayed the combination of the visuospatial and motor features that were revealed by the memory tasks. When aligned to the presentation of the visual target, the activity profiles were characterized by 2 main peaks that had the same latency of the visual and motor ones observed in the memory tasks. This suggests that the formation of these profiles resides on a common mechanism that is independent both from the effector used for action and from the presence of the visual IS, therefore, from the specific task adopted. In fact, the motor peak emerged with same timing not only for movement to visual targets but also for movement to memorized locations.

The presence of distinguishable visuospatial and motor peaks in the population profiles of area 7a is reminiscent of what observed by Schall (1991) in the frontal eye fields (FEF), and this is not surprising provided that parietal area 7a and area 8Ac in the FEF are linked by corticocortical connections (Schall and others 1995).

To compare neural properties across different compartments of posterior parietal cortex, we have also used data from previous experiments (Battaglia-Mayer and others 2000, 2001) performed in SPL (areas V6A and PEc). In this case, the population activities during reaching, reach-fix, and saccade tasks had identical shape and timing. They were characterized by a single peak, occurring at 235 ms after presentation of the visual target serving as Go signal. This peak occurred within the hand RT and the end of the saccade, whereas the entire population activity lasted about 800 ms after target presentation, independently from the effector set in motion. The temporal profile of the population activity remained unchanged when the position of the eye changed, suggesting that in SPL this profile mostly reflects the hand motor behavior, as also confirmed by the much weaker population activity obtained during eye movement only.

In both SPL and IPL, the temporal span of the population activity was similar, although the activation relative to hand movement was stronger and about 200 ms earlier in the former than in the latter, suggesting that SPL can be a source of input signals to IPL via intraparietal connections (Rozzi and others 2005).

These observations suggest that the parietal lobe contains a common neural mechanism for eye and hand movement control, as indicated by the temporal dynamics of neural activity, that takes into account both visual target localization and eye–hand action. In both SPL and IPL, this control mechanism seems largely independent of the effector used and might be based on a temporal dimension on which different and composite action can synchronize. The exact nature of this control remains to be determined. However, this mechanism can be the neural basis of the temporal coupling between eye and hand movement, for which overwhelming evidence exists in the psychophysical literature (for instance, see Biguer and others 1982; Fisk and Goodale 1985; Vercher and others 1994; Sailer and others 2000; Binsted and others 2001; Ariff and others 2002; Neggers and Bekkering 2002). We can also speculate that, in spite of their different timing of action, this mechanism might provide a common temporal input drive to the eye and the hand control systems, to account for planning, execution, and online adjustments. This interpretation is

supported by a Transcranial Magnetic Stimulation study (van Donkelaar and others 2000) showing that transient inactivation of parietal cortex prior to the onset of saccadic eye movement disrupts the natural correlation between eye and hand movement amplitude during reaching.

The results of this study might help the interpretation of motor disorders of parietal patients from a physiological perspective. Lesion of the right IPL in humans causes hemispatial neglect that is characterized by both perceptual and motor disorders. The hallmark of the latter is directional hypokinesia (Watson and others 1978; Heilman and others 1985; Mattingley and others 1992, 1998; Husain and others 2000) that consists in an elongation of RT and movement time for leftward reaches, with either hand. Parietal patients display similar disorders in the oculomotor domains, so that leftward saccades to visual targets are delayed, hypometric, and of "staircase" type (Girotti and others 1983; Pierrot-Deseilligny and others 1991; Husain and Rorden 2003; Niemeier and Karnath 2003). In monkeys, lesions centered on the IPL result in errors in visually guided reaching (for a review, see Battaglia-Mayer and others 2005). The disorder consists in an elongation of RT and movement time of both arms to contralesional targets (Faugier-Grimaud and others 1985), a syndrome closely resembling directional hypokinesia in neglect patients. In monkeys, parietal lesions also result in attentional and saccadic eye movement disorders (Lynch and McLaren 1989).

A previous study (Battaglia-Mayer and others 2005) of area 7a has shown a marked anisotropy in the distribution of cells' preferred directions computed during eye and/or hand RT and movement time, because most of them pointed toward the contralateral hemispace. It has been proposed that the movement disorders typical of directional hypokinesia can be consequence of the loss of neuronal populations encoding directional motor space in such anisotropic fashion. The results of the present manuscript, by showing how the population activities preceding eye, hand, or coordinated eye–hand movements show similar temporal evolution and profiles, suggest the existence in area 7a of a mechanism for control of eye–hand movement whose collapse might be responsible for the movement disorders typical of parietal patients.

Supplementary Material

Supplementary material can be found at: http://www.cercor. oxfordjournals.org/.

Notes

Address correspondence to Prof Alexandra Battaglia-Mayer, Dipartimento di Fisiologia umana e Farmacologia, Università di Roma "La Sapienza," Piazzale Aldo Moro 5, 00185 Rome, Italy. Email: alexandra. battagliamayer@uniroma1.it.

References

Andersen RA. 1995. Encoding of intention and spatial location in the posterior parietal cortex. Cereb Cortex 5:457–469.

Andersen RA, Bracewell RM, Barash S, Gnadt JK, Fogassi L. 1990. Eye position effects on visual, memory, and saccade-related activity in areas LIP and 7a of Macaque. J Neurosci 10:1176–1196.

Andersen RA, Mountcastle VB. 1983. The influence of the angle of gaze upon the excitability of the light-sensitive neurons of the posterior parietal cortex. J Neurosci 3:532–548.

Ariff G, Donchin O, Nanayakkara T, Shadmehr R. 2002. A real-time predictor in motor control: study of saccadic eye movements during unseen reaching movements. J Neurosci 22:7721–7729.

Averbeck BB, Chafee MV, Crowe DA, Georgopoulos AP. 2005. Parietal representation of hand velocity in a copy task. J Neurophysiol 93:508–518.

Barash S, Bracewell RM, Fogassi L, Gnadt JW, Andersen RA. 1991. Saccade-related activity in the lateral intra-parietal area (LIP). I. Temporal properties; comparison to area 7a. J Neurophysiol 66:1095–1108.

Battaglia-Mayer A, Caminiti R, Lacquaniti F, Zago M. 2003. Multiple levels of representation of reaching in the parieto-frontal network. Cereb Cortex 13:1009–1022.

Battaglia-Mayer A, Ferraina S, Genovesio A, Marconi B, Squatrito S, Lacquaniti F, Caminiti R. 2001. Eye-hand coordination during reaching. II. An analysis of the relationships between visuomanual signals in parietal cortex and parieto-frontal association projections. Cereb Cortex 11:528–544.

Battaglia-Mayer A, Ferraina S, Mitsuda T, Marconi B, Genovesio A, Onorati P, Lacquaniti F, Caminiti R. 2000. Early coding of reaching in the parieto-occipital cortex. J Neurophysiol 83:2374–2391.

Battaglia-Mayer A, Mascaro M, Brunamonti E, Caminiti R. 2005. The over-representation of contralateral space in parietal cortex: a positive image of directional motor components of neglect? Cereb Cortex 15:514–525.

Batista AP, Buneo CA, Snyder LH, Andersen RA. 1999. Reach plans in eye-centered coordinates. Science 285:257–260.

Biguer B, Jeannerod M, Prablanc C. 1982. The coordination of eye, head, and arm movements during reaching at a single visual target. Exp Brain Res 46:301–304.

Binsted G, Chua R, Helsen W, Elliott D. 2001. Eye-hand coordination in goal-directed aiming. Hum Mov Sci 20:563–585.

Blum B. 1985. Manipulation reach and visual reach neurons in the inferior parietal lobule of the rhesus monkey. Behav Brain Res 18:167–173.

Bushnell MC, Goldberg ME, Robinson DL. 1981. Behavioral enhancement of visual responses in monkey cerebral cortex. I. Modulation in posterior parietal cortex related to selective visual attention. J Neurophysiol 46:755–772.

Calton JL, Dickinson AR, Snyder LH. 2002. Non-spatial, motor specific activation in posterior parietal cortex. Nat Neurosci 5:580–588.

Constantinidis C, Steinmetz MA. 1996. Neuronal activity in posterior parietal area 7a during the delay periods of a spatial memory task. J Neurophysiol 76:1352–1355.

Constantinidis C, Steinmetz MA. 2001. Neuronal responses in area 7a to multiple-stimulus displays: I. Neurons encode the location of the salient stimulus. Cereb Cortex 11:581–591.

Constantinidis C, Steinmetz MA. 2005. Posterior parietal cortex automatically encodes the location of salient stimuli. J Neurosci 25:233–238.

Faugier-Grimaud S, Frenois C, Peronnet F. 1985. Effects of posterior parietal lesions on visually guided movements in monkeys. Exp Brain Res 59:125–138.

Ferraina S, Garasto MR, Battaglia-Mayer A, Ferraresi P, Johnson PB, Lacquaniti F, Caminiti R. 1997. Visual control of hand reaching movement: activity in parietal area 7m. Eur J Neurosci 9:1090–1095.

Ferraina S, Johnson PB, Garasto MR, Battaglia-Mayer A, Ercolani L, Bianchi L, Lacquaniti F, Caminiti R. 1997. Combination of hand and gaze signals during reaching: activity in parietal area 7m in the monkey. J Neurophysiol 77:1034–1038.

Fisk JD, Goodale MA. 1985. The organization of eye and limb movements during unrestricted reaching to targets in contralateral and ipsilateral visual space. Exp Brain Res 60:159–178.

Girotti F, Casazza M, Musicco M, Avanzini G. 1983. Oculomotor disorders in cortical lesions in man: the role of unilateral neglect. Neuropsychologia 21:543–553.

Gottlieb JP, Kusunoki M, Goldberg ME. 1998. The representation of visual salience in monkey parietal cortex. Nature 391:481–484.

Heilman KM, Bowers D, Coslett HB, Whelan H, Watson RT. 1985. Directional hypokinesia: prolonged reaction times for leftwards movements in patients with right hemisphere lesions and neglect. Neurology 35:855–859.

Husain M, Mattingley JB, Rorden C, Kennard C, Driver J. 2000. Distinguishing sensory and motor biases in parietal and frontal neglect. Brain 123:1643–1659.

Husain M, Rorden C. 2003. Non-spatially lateralized mechanisms in hemispatial neglect. Nat Rev Neurosci 4:26–36.

Hyvärinen J, Poranen A. 1974. Function of the parietal associative area 7 as revealed from cellular discharges in alert monkeys. Brain 97:673–692.

Lacquaniti F, Guigon E, Bianchi L, Ferraina S, Caminiti R. 1995. Representing spatial information for limb movement: role of area 5 in the monkey. Cereb Cortex 5:391–409.

Lynch JC, McLaren JW. 1989. Deficits of visual attention and saccadic eye movements after lesions of parietoocippital cortex in monkeys. J Neurophysiol 61:74–90.

Lynch JC, Mountcastle VB, Talbot WH, Yin TC. 1977. Parietal lobe mechanisms for directed visual attention. J Neurophysiol 40:362–389.

MacKay WA. 1992. Properties of reach-related neuronal-activity in cortical area 7a. J Neurophysiol 67:1335–1345.

Mattingley JB, Bradshaw JL, Phillips JG. 1992. Impairments of movement initiation and execution in unilateral neglect. Brain 115:1849–1874.

Mattingley JB, Husain M, Rorden C, Kennard C, Driver J. 1998. Motor role of the human inferior parietal lobe revealed in unilateral neglect patients. Nature 392:179–182.

Merchant H, Battaglia-Mayer A, Georgopoulos AP. 2001. Effects of optic flow in motor cortex and area 7a. J Neurophysiol 86:1937–1954.

Motter BC, Mountcastle VB. 1981. The functional properties of light-sensitive neurons of the posterior parietal cortex studied in waking monkeys: foveal sparing and opponent vector organization. J Neurosci 1:3–26.

Mountcastle VB. 1995. The parietal system and some higher brain functions. Cereb Cortex 5:377–390.

Mountcastle VB, Andersen R, Motter BC. 1981. The influence of attentive fixation upon the excitability of light-sensitive neurons of the posterior parietal cortex. J Neurosci 1:1218–1225.

Mountcastle VB, Lynch JC, Georgopoulos AP, Sakata H, Acuña C. 1975. Posterior parietal association cortex of the monkey: command functions for operations within extrapersonal space. J Neurophysiol 38:871–908.

Neggers SFW, Bekkering H. 2002. Coordinated control of eye and hand movements in dynamic reaching. Hum Mov Sci 21:37–64.

Niemeier M, Karnath HO. 2003. Stimulus-driven and voluntary saccades are coded in different coordinate systems. Curr Biol 13:585–589.

Pandya DN, Seltzer B. 1982. Intrinsic connections and architectonics of posterior parietal cortex in the rhesus monkey. J Comp Neurol 204:196–210.

Pierrot-Deseilligny C, Rivaud S, Gaymard B, Agid Y. 1991. Cortical control of reflexive visually-guided saccades. Brain 114:1473–1485.

Richmond BJ, Optican LM, Spitzer H. 1990. Temporal encoding of two-dimensional patterns by single units in primate primary visual cortex. I. Stimulus-response relations. J Neurophysiol 64:351–369.

Robinson DL, Goldberg ME, Stanton GB. 1978. Parietal association cortex in the primate: sensory mechanisms and behavioral modulations. J Neurophysiol 41:910–932.

Rozzi S, Calzavara R, Belmalih A, Borra E, Gregoriou GG, Matelli M, Luppino G. 2005. Cortical connections of the inferior parietal cortical convexity of the macaque monkey. Cereb Cortex. doi:10.1093/cercor/bhj076.

Sailer U, Eggert T, Ditterich J, Straube A. 2000. Spatial and temporal aspects of eye-hand coordination across different tasks. Exp Brain Res 134:163–173.

Schall JD. 1991. Neural activity related to visually guided saccades in the frontal eye fields of reshus monkeys: comparison with supplementary eye fields. J Neurophysiol 66:559–597.

Schall JD, Morel A, King DJ, Bullier J. 1995. Topography of visual cortex connections with frontal eye field in macaque: convergence and segregation of processing streams. J Neurosci 15:4464–4487.

Snyder LH, Batista AP, Andersen RA. 1997. Coding of intention in the posterior parietal cortex. Nature 386:167–170.

van Donkelaar P, Lee J-H, Drew AS. 2000. Transcranial magnetic stimulation disrupts eye-hand interactions in the posterior parietal cortex. J Neurophysiol 84:1677–1680.

Vercher JL, Magenes G, Prablanc C, Gauthier GM. 1994. Eye-head-hand coordination in pointing at visual targets: spatial and temporal analysis. Exp Brain Res 99:507–523.

Watson RT, Miller BD, Heilman KM. 1978. Nonsensory neglect. Ann Neurol 3:505–508.